Supplementary Figures

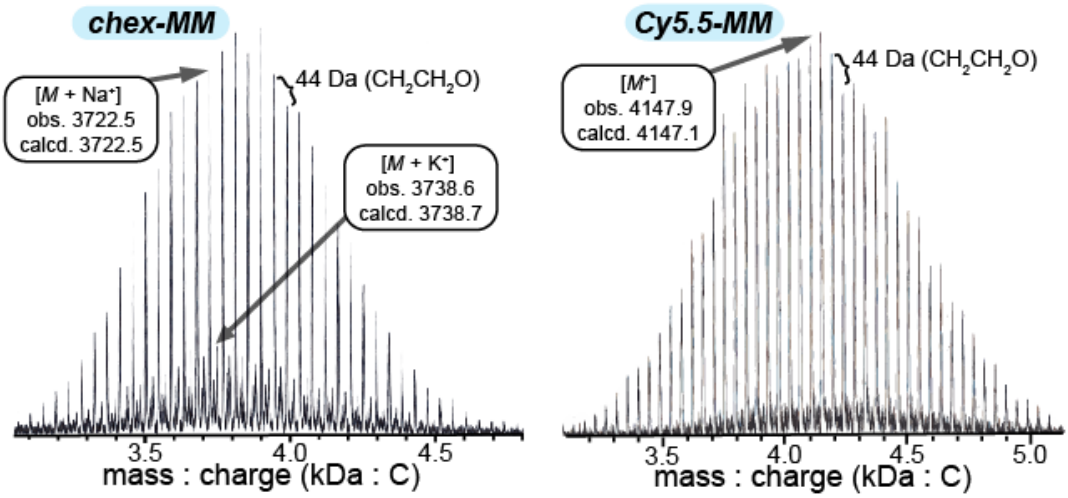

Supplementary Figure 1. MALDI-TOF spectra of chex-MM and Cy5.5-MM. Observed and calculated masses are provided.

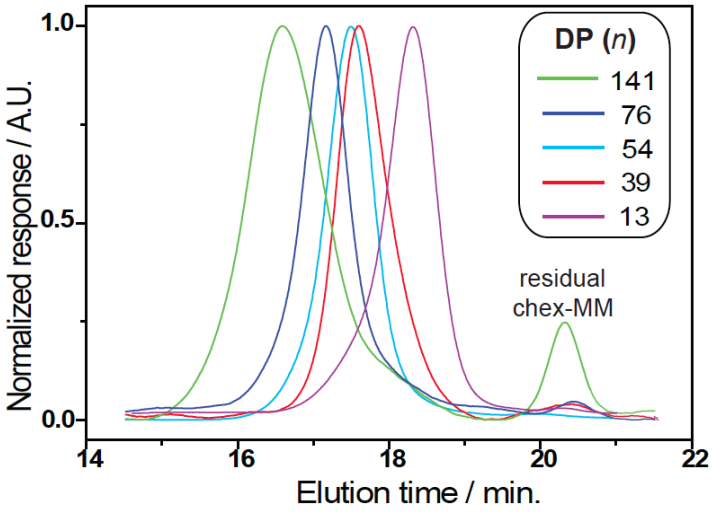

Supplementary Figure 2. GPC analysis of branched bottlebrush polymers prepared from chex-MM. GPC traces of several polymers derived from chex-MM with various average degrees of polymerization, *n*, prior to dialysis. Only the *n* = 141 sample shows a significant amount of residual macromonomer.

	r_1	r_2
P1	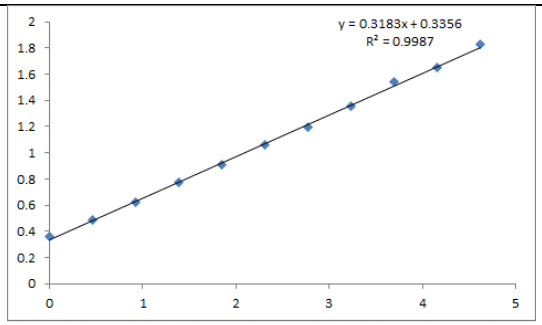	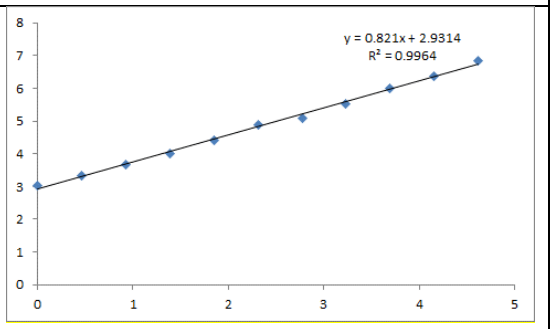

Supplementary Figure 3. **Relaxivity plots.** Typical plots of $1/T_1$ and $1/T_2$ vs concentration of nitroxide (mM) for polymer P1. The slopes provide relaxivities r_1 and r_2.

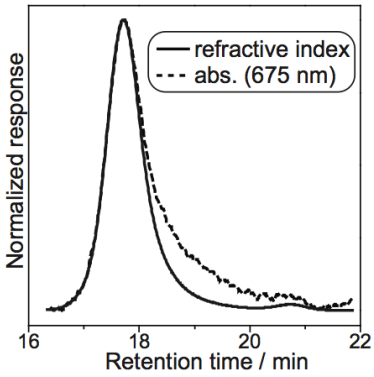

Supplementary Figure 4. GPC Analysis of OF1. Refractive index and 675 nm absorbance GPC traces of OF1. The overlap of the two spectra supports the formation of a copolymer of chex-MM and Cy5.5-MM.

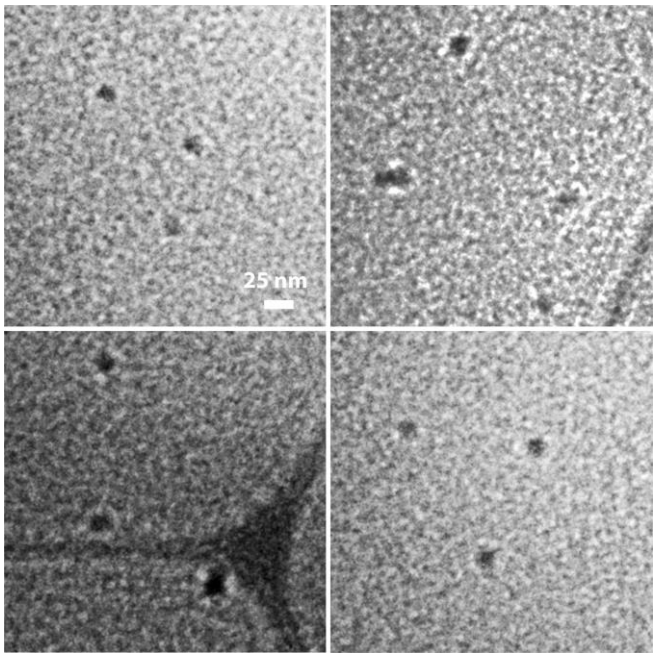

Supplementary Figure 5. **Cryo-TEM analysis of OF1.** Cryogenic transmission electron microscopy (cryo-TEM) image of OF1.

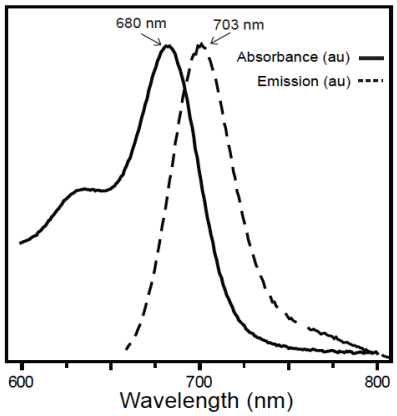

Supplementary Figure 6. **Excitation and emission spectra for OF1.** The spectra confirm the presence of Cy5.5 in OF1.

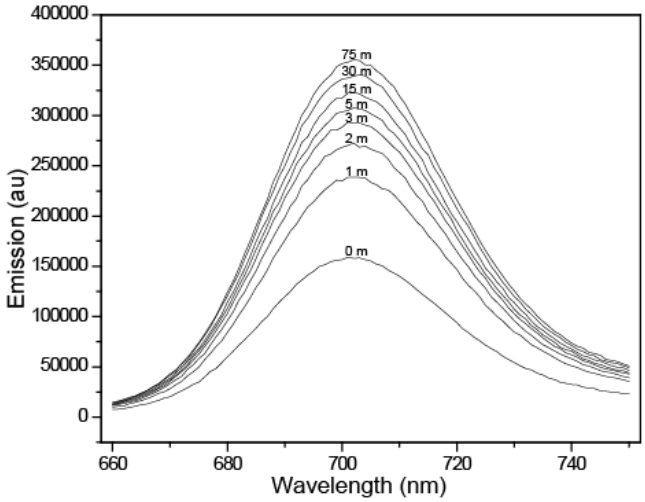

Supplementary Figure 7. Fluorescence emission spectra versus time for OF1 treated with ascorbate. Representative emission spectra for OF1 before and after exposure to ascorbate. Ascorbate-induced nitroxide reduction leads to enhanced Cy5.5 emission over 75 minutes.

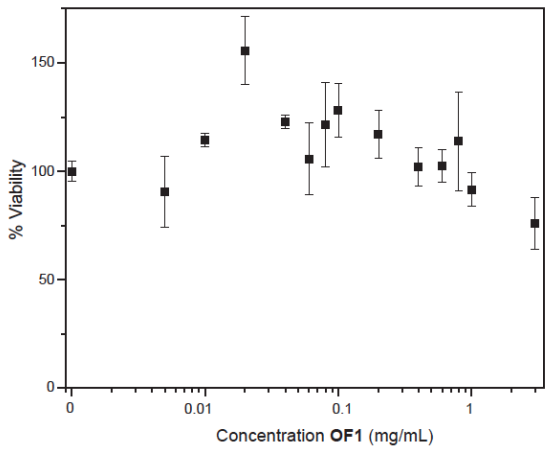

Supplementary Figure 8. ***In vitro*** **cytotoxicity.** HeLa cell viability in the presence of OF1 as measured by MTT assay. No discernable toxicity was observed up to 3 mg/mL.

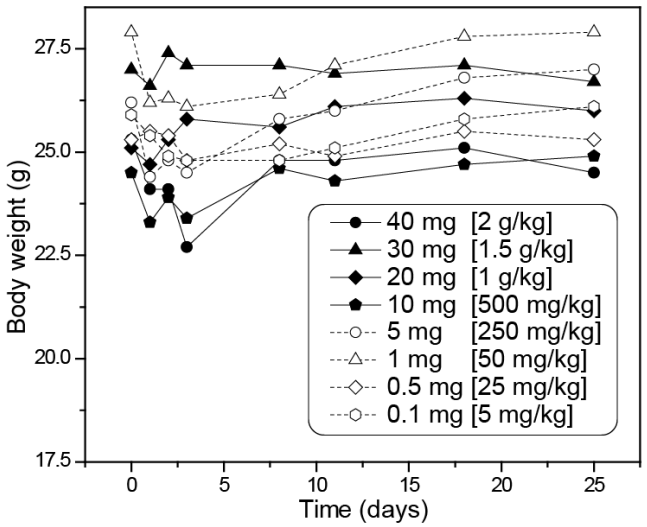

Supplementary Figure 9. *In vivo* gross toxicity. Mouse weight as a function of time after injection of varied doses (5 mg – 2 g / kg animal) of OF1.

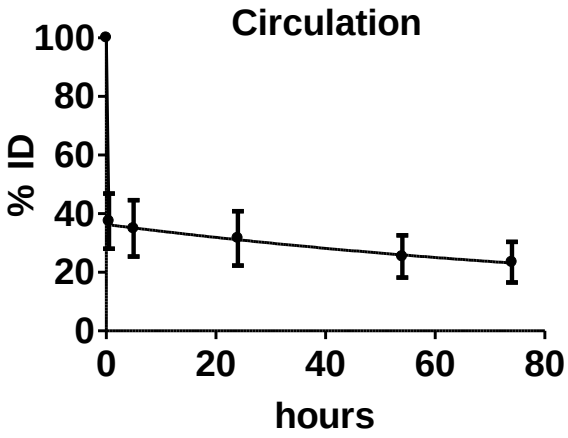

Supplementary Figure 10. *In vivo* pharmacokinetic analysis of OF1. A blood draw of 0.05 mL was taken at each time point and subjected to fluorescence imaging via IVIS. Measurements were repeated in triplicate and compared to the amount of injected fluorescence (100%). The data were fit to a two-compartment model following standard procedures.[1]

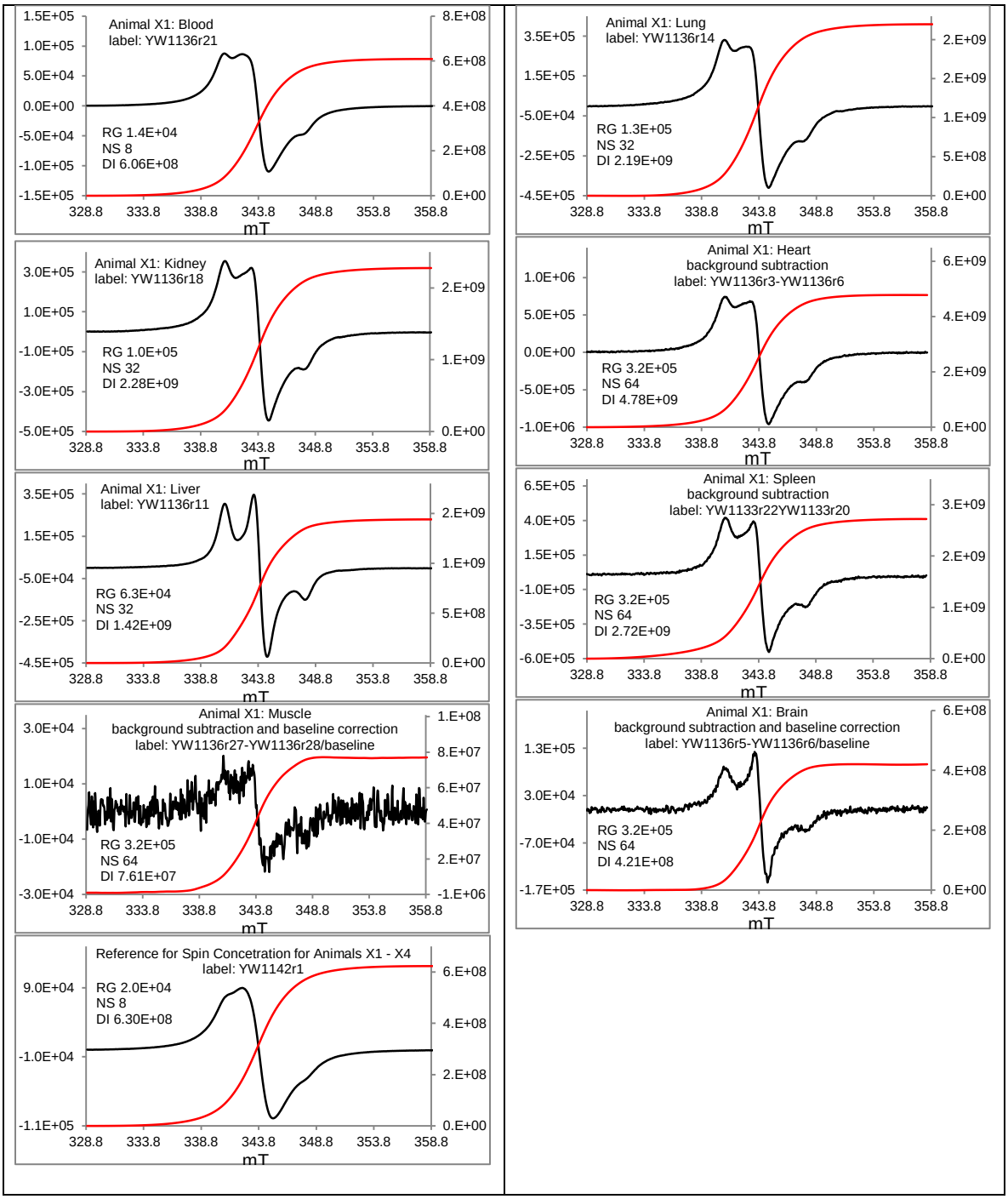

Supplementary Figure 11. *Ex* vivo EPR analyses. *Ex vivo* EPR spectra (black) with double integration lines (red) for animal X1 and the reference for spin concentration (bottom spectrum). All spectra were measured at –30 °C (243.2 K). Left and right vertical axes correspond to the peak height and double integrated (DI) intensity scales, respectively; RG = receiver gain, NS = number of scans.

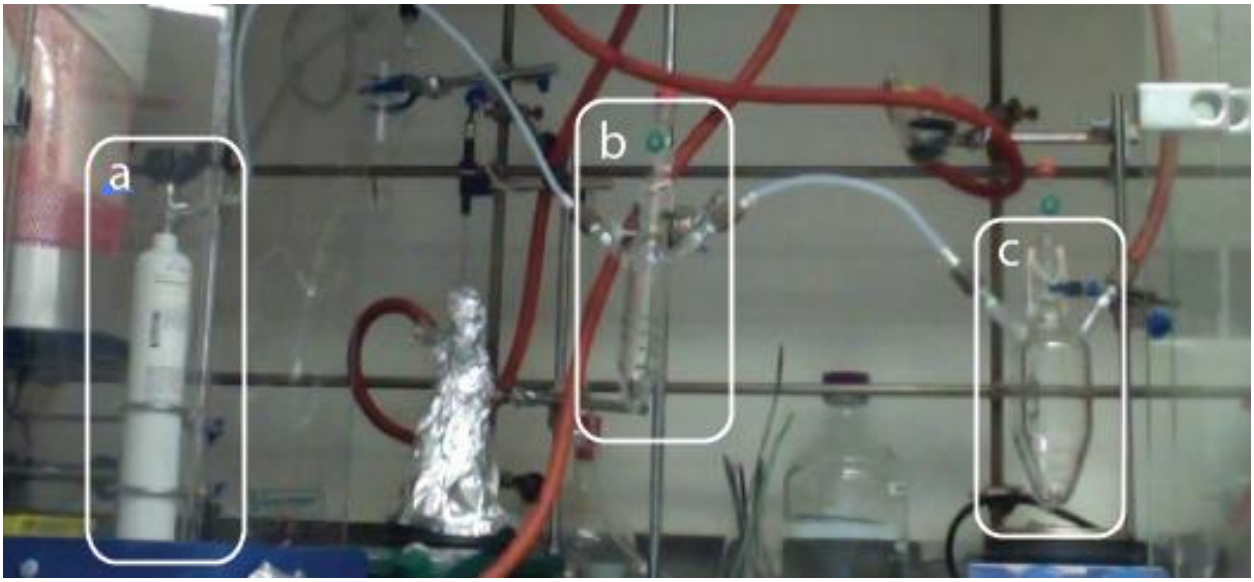

Supplementary Figure 12. Ethylene oxide (EO) polymerization setup for the synthesis of PEG-amine (PEG-NH_2). (a) EO tank, (b) EO drying vessel, and (c) reaction flask equipped with Pyrex coated stir bar.

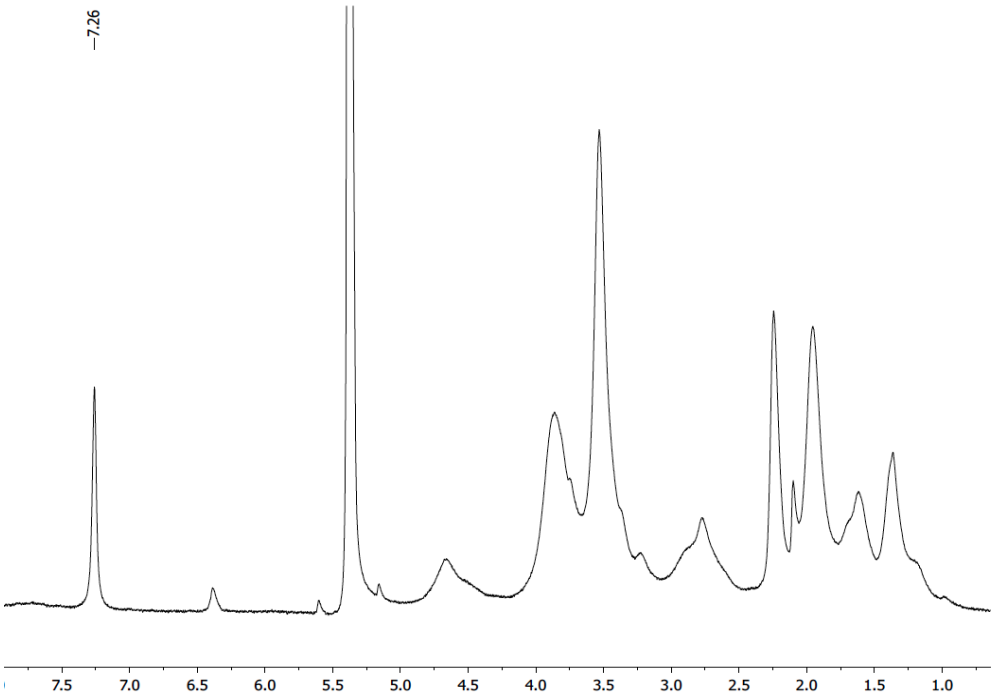

Supplementary Figure 13. ^{1}H NMR (400 MHz, $CDCl_3$, r.t.) spectrum for azide 3.

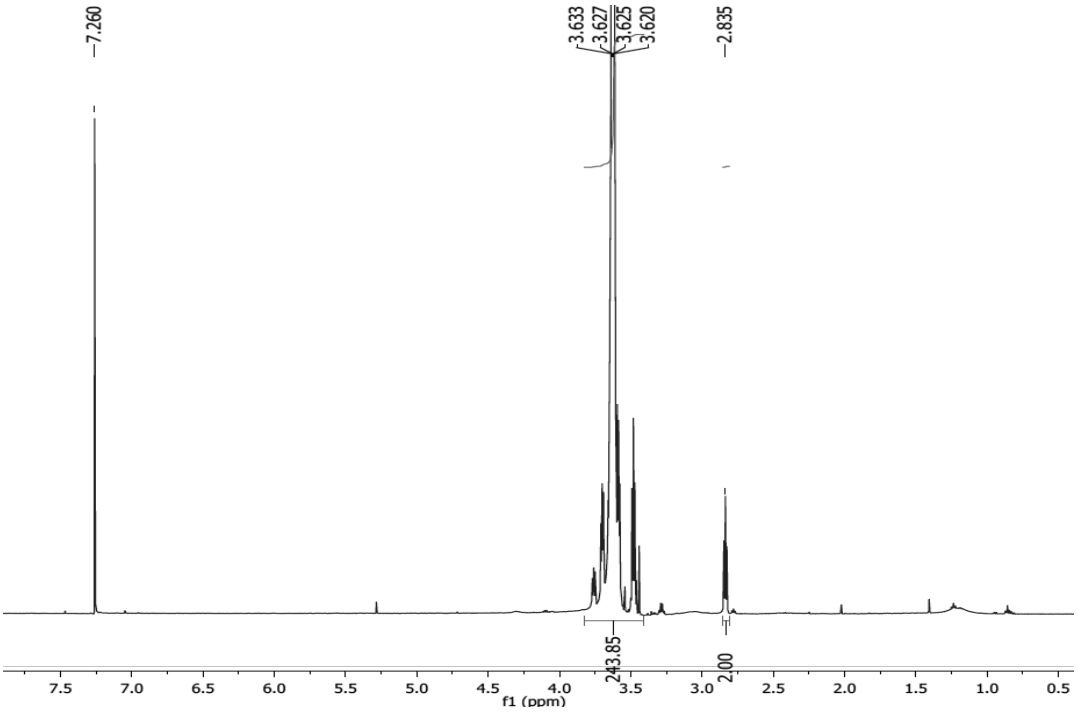

Supplementary Figure 14. ^{1}H NMR (400 MHz, $CDCl_3$, r.t.) spectrum for PEG-NH_2.

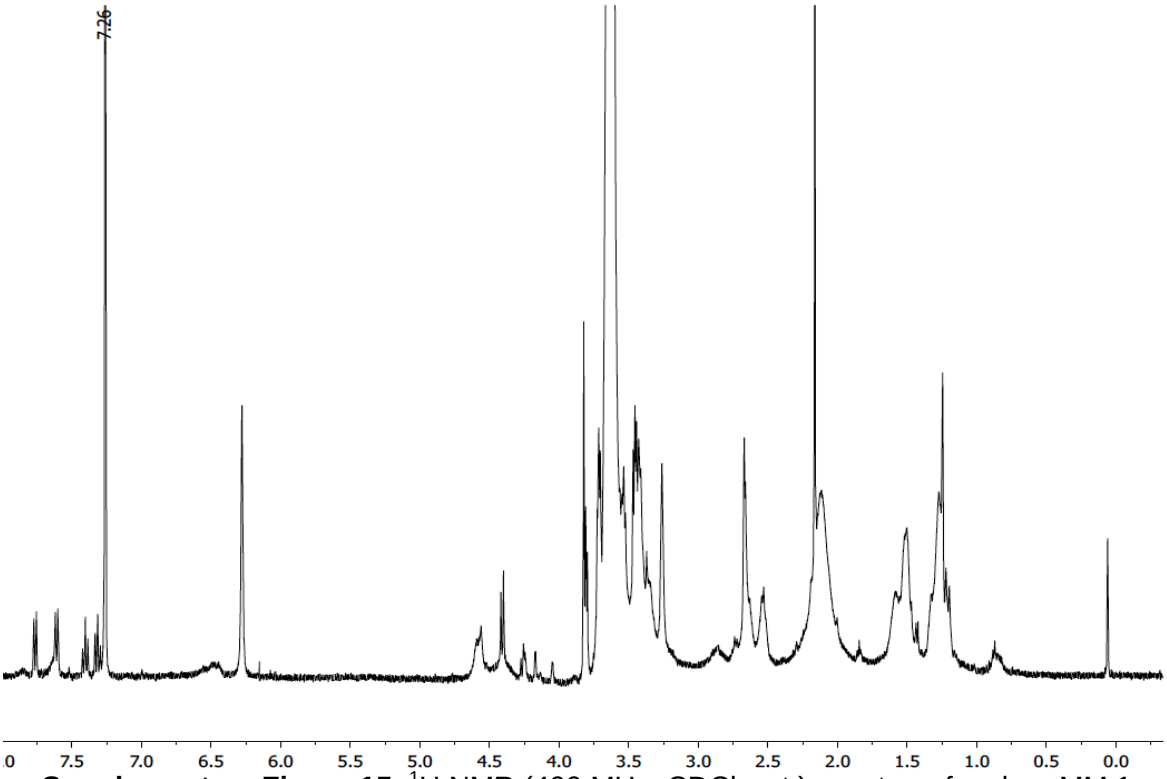

Supplementary Figure 15. ^{1}H NMR (400 MHz, $CDCl_3$, r.t.) spectrum for chex-MM 1.

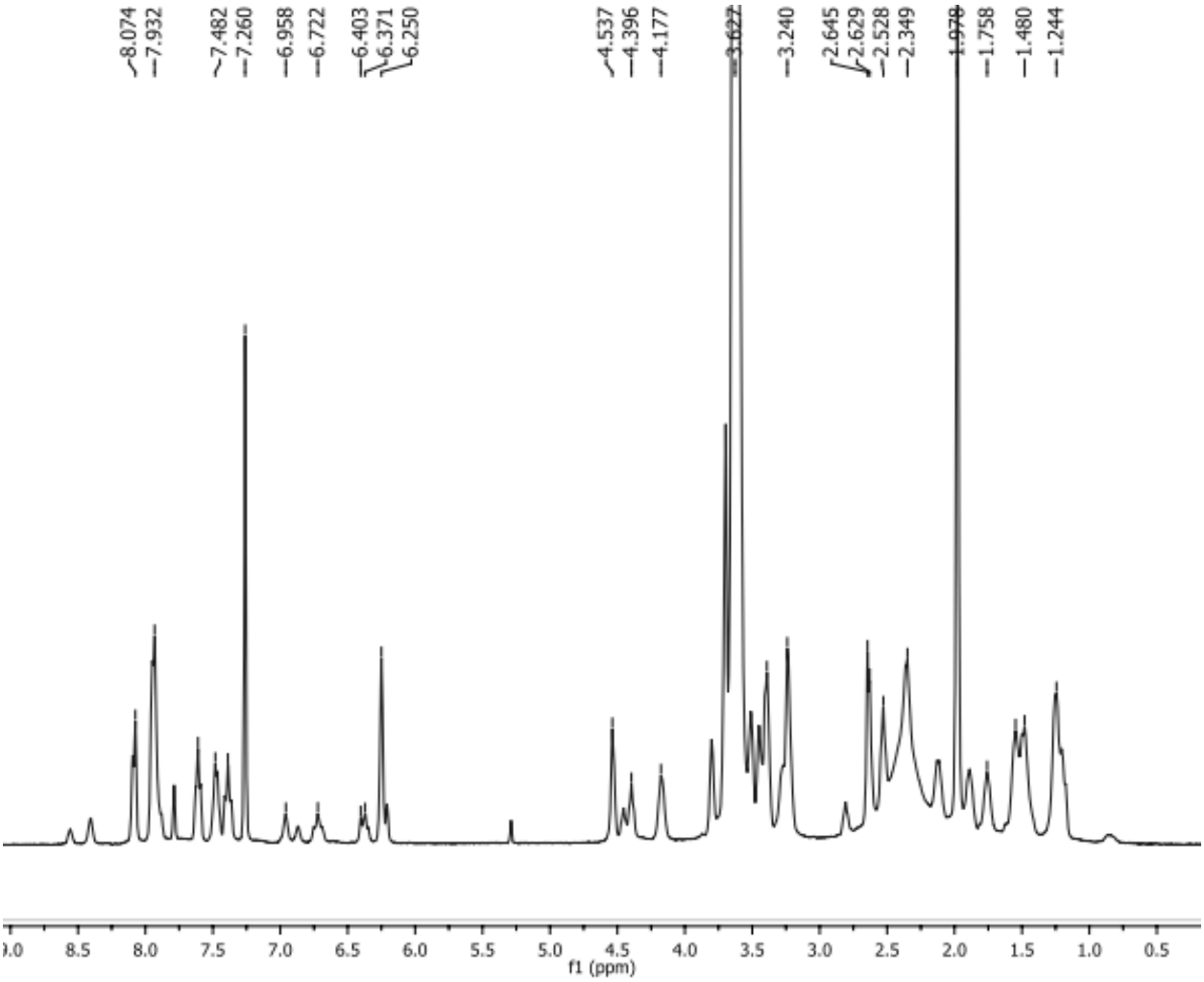

Supplementary Figure 16. ^{1}H NMR (400 MHz, $CDCl_3$, r.t.) spectrum for Cy5.5-MM 2.

Supplementary Tables

n	*Đ*	D_H *(nm)*	*r1 ($mM^{-1}s^{-1}$)*	*r2 ($mM^{-1}s^{-1}$)*
n.a. (chex-MM)	1.02	-	0.21	0.30
13	1.03	11.8	0.31	0.55
39	1.02	14.6	0.32	0.70
54	1.05	16.8	0.32	0.82
76	1.08	18.0	0.36	0.84
141	1.30	21.0	0.31	0.51
proxyl	1.00	-	0.15	0.17
dendrimer	1.00	-	0.44	0.86

Supplementary Table 1. Branched bottlebrush polymer characterization. Dispersity (GPC), hydrodynamic radius (DLS), and r_1 and r_2 relaxation parameters for samples with varying degrees of polymerization (*n*). Proxyl refers to 3-carboxy-proxyl, and "dendrimer" refers to Rajca'a previously studied polypropylenimine (PPI) nitroxide-conjugated fourth generation dendrimer.

Sample Label	Spin Conc. (%)	Data Label	Nitrox. Conc. (mM)	Asc. Conc. (mM)	GSH Conc. (mM)	Decay Time (s)	Line Width Init. (G)	Line Width Fin. (G)	Decay in Expt. (%)	Initial Kinetics Range of Fit (s)	Initial Kinetics k' (s^{-1})	Initial Kinetics R^2	Initial Kinetics k ($M^{-1}s^{-1}$)	Initial Kinetics Avg k ($M^{-1}s^{-1}$)	Late Kinetics Range of Fit (s)	Late Kinetics k' (s^{-1})	Late Kinetics R^2	Late Kinetics k ($M^{-1}s^{-1}$)
TEMPO-conjugated branched-bottlebrush polymer[2]	93	YW960	0.125	2.5	0	283	3.1	2.7	66	83–243	7.27×10^{-3}	0.9933	2.91×10^{0}	3.00	/	/	/	/
		YW960-2	0.125	2.5	0	229	3.1	2.9	55	69–189	7.72×10^{-3}	0.9984	3.09×10^{0}		/	/	/	/
		YW961	0.125	2.5	1.25	295	3.1	3.0	70	95–255	8.73×10^{-3}	0.9967	3.49×10^{0}	/	/	/	/	/
chex-MM	93	YW947	0.2	4.0	0	600	/	/	27	77–600	5.17×10^{-4}	0.9922	1.29×10^{-1}	1.26×10^{-1}	/	/	/	/
		YW962	0.125	2.5	0	3000	4.5	4.5	51	162–702	3.05×10^{-4}	0.9963	1.22×10^{-1}		1072–3000	1.65×10^{-4}	0.9883	6.58×10^{-2}
		YW963	0.125	2.5	1.25	3000	4.6	4.6	52	169–889	3.15×10^{-4}	0.9963	1.26×10^{-1}	/	979–3000	1.88×10^{-4}	0.9861	7.50×10^{-2}
P1	83	YW981	0.50	10.0	0	1811	5.8	6.9	41	251–851	2.66×10^{-4}	0.9778	2.66×10^{-2}	2.71×10^{-2}	971–1811	9.42×10^{-5}	0.9233	9.42×10^{-3}
		YW985	0.50	10.0	0	10800	6.4	6.8	51	278–878	2.75×10^{-4}	0.9780	2.75×10^{-2}		3600–10800	1.75×10^{-5}	0.9789	1.75×10^{-3}
		YW982	0.50	10.0	5.0	1857	6.2	6.8	40	177–897	2.61×10^{-4}	0.9604	2.61×10^{-2}	2.77×10^{-2}	1137–1857	1.15×10^{-4}	0.8916	1.15×10^{-2}
		YW983	0.50	10.0	5.0	10800	6.2	6.9	61	396–1019	2.93×10^{-4}	0.9942	2.93×10^{-2}		3600–10800	3.73×10^{-5}	0.9864	3.73×10^{-3}
dendrimer[3]	/	JP609	0.50	10.0	0	>3600	/	/	/	90–390	6.20×10^{-4}	0.9810	6.20×10^{-2}	$5.8 \pm 0.4\times10^{-2}$	4500–10800	2.92×10^{-5}	0.9874	2.92×10^{-3}
		JP610	0.50	10.0	0	<3600	/	/	/	115–415	5.42×10^{-4}	0.9766	5.42×10^{-2}		/	/	/	/
		JP611	0.50	10.0	0	<3600	/	/	/	126–426	5.73×10^{-4}	0.9985	5.73×10^{-2}		/	/	/	/

Supplementary Table 2. Nitroxide reduction kinetics data. Ascorbate and glutathione (GSH) quenching kinetics for chex-MM, P1, a TEMPO-conjugated branched bottlebrush polymer[2], and Rajca's nitroxide-conjugated PPI dendrimer[3]. Throughout the *ex vivo* EPR spectroscopy section, labels "YW1133r3-6" and alike correspond to sample or experiment codes directly traceable to the laboratory notebooks or raw data.

Animal (weight, g)	Sample	Weight of Tissue (mg)	PBS Added (μL)	Volume of Tissue Mixture (mL)	Spin Conc (mixture) (μM)	Spin Conc (tissue) (μmol/g)	*g*	EPR Data Label
X1 (23.8)	Brain	285.5	400	685.5	5.35	0.0128	2.005	YW1136r5
	Liver	1534.2	300	1834.2	185.1	0.2213	2.005	YW1136r11-12
	Kidney	453.7	400	853.7	185.1	0.3483	2.005	YW1136r18-19
	Lung	179.4	400	579.4	143.2	0.4625	2.006	YW1136r14-15
	Heart	140.0	400	540	60.88	0.2348	2.005	YW1136r3
	Muscle	15.1	400	415.1	0.68	0.0187	2.005	YW1136r27
	Spleen	111.8	400	511.8	34.64	0.1586	2.005	YW1136r7
	Tumor	147.3	400	547.3	6.14	0.0228	2.005	YW1136r25
	Blood		0		1385.9	1.3859	2.006	YW1136r21-22
X2 (26.7)	Brain	361.9	400	761.9	17.28	0.0364	2.005	YW1137r5
	Liver	1463.0	400	1863	80.33	0.1023	2.005	YW1137r11-12
	Kidney	397.1	400	797.1	223.7	0.4490	2.006	YW1137r20-21
	Lung	197.9	400	597.9	194.5	0.5876	2.005	YW1137r17-18
	Heart	129.4	400	529.4	73.24	0.2996	2.005	YW1137r3
	Muscle	37.8	400	437.8	1.82	0.0211	2.006	YW1137r29
	Spleen	104.6	400	504.6	37.64	0.1816	2.005	YW1137r7
	Tumor	142.9	400	542.9	3.48	0.0132	2.006	YW1137r27
	Blood		0		1489.2	1.4892	2.005	YW1137r22-23
X3 (28.8)	Brain	380.4	400	780.4	12.64	0.0259	2.005	YW1133r9
	Liver	1801.0	300	2101	120.2	0.1402	2.005	YW1133r12-13
	Kidney	492.8	400	892.8	133.9	0.2426	2.005	YW1133r30-31
	Lung	209.8	400	609.8	139.1	0.4043	2.006	YW1133r25-26
	Heart	133.1	400	533.1	50.27	0.2013	2.005	YW1133r17
	Muscle	54.1	400	454.1	5.03	0.0422	2.006	YW1133r44
	Spleen	137.5	400	537.5	38.20	0.1493	2.006	YW1133r22
	Tumor	323.7	400	723.7	17.01	0.0380	2.006	YW1133r40
	Blood		0		1824	1.824	2.006	YW1133r34-36
X4 (25.4)	Brain	284.0	400	400	7.64	0.0184	2.005	YW1138r5
	Liver	1603.4	400	400	155.1	0.1938	2.005	YW1138r11-12
	Kidney	493.7	400	400	125.1	0.2265	2.006	YW1138r18-19
	Lung	190.0	400	400	131.5	0.4083	2.006	YW1138r14-15
	Heart	130.9	400	400	37.27	0.1512	2.005	YW1138r3
	Muscle	11.3	400	411.3	1.69	0.0615	2.006	YW1138r28
	Spleen	152.0	400	400	22.00	0.0799	2.005	YW1138r7
	Tumor	41.9	400	441.9	6.28	0.06623	2.005	YW1138r26
	Blood		0		1408.7	1.4087	2.006	YW1138r21-23

Supplementary Table 3. *Ex vivo* tissue analysis. Summary of spin concentration measurements for animals X1, X2, X3, and X4 by *ex-vivo* EPR spectroscopy. Tissues were collected 0.5 h after injection of 30-mg dose (7.9 μmol of nitroxide radical) of polymer (DP = 48, MW ≈ 180 kDa, containing 1% wt fluorophore).

Supplementary Notes

Supplementary Note 1. Instrumentation information. ^{1}H nuclear magnetic resonance (^{1}H NMR) spectra were obtained from Bruker AVANCE-400 NMR spectrometers at MIT. NMR spectra were analyzed using MestReNova NMR 8.0.1 software and referenced to the residual chloroform peak at 7.26 ppm. Electron Paramagnetic Resonance (EPR) spectra were obtained at the University of Nebraska using a Bruker CW X-band spectrometer, equipped with a frequency counter. The spectra were obtained using a dual mode cavity; all spectra were recorded using an oscillating magnetic field perpendicular (TE_{102}) to the swept magnetic field. DPPH powder (g = 2.0037) was used as a g-value reference. Gel permeation chromatography (GPC) analysis was performed on an Agilent 1260 LC system equipped with an Agilent multi-wavelength UV/Vis detector, Wyatt T-rEX refractive index detector, Wyatt DAWN EOS 18-angle light scattering detector, and two Shodex KD-806M GPC columns. The GPC system was equilibrated at 60 °C with a 1 mL/min flow rate of DMF with 0.025 M LiBr. Dynamic light scattering (DLS) measurements were taken at room temperature using a Wyatt Technology DynaPro Titan DLS. Samples were dissolved in phosphate buffered saline solution, passed through a 0.4 μm nylon syringe filter into a 0.3 mm cuvette. Average hydrodynamic radii were obtained using Dynamics V6 software from DynaPro Wyatt Technologies. DLS correlation curves were fit using the CONTIN algorithm. Matrix-assisted laser desorption/ionization time-of-flight (MALDI-TOF) analyses were collected on a Bruker OmniFlex instrument with a 337 nm N_2 laser with a 0.1 nm spectral bandwidth. Liquid chromatography-mass spectrometry (LC-MS) data were obtained on an Agilent 1260 LC system with an Agilent 6130 single quadrupole mass spectrometer. Separation was achieved using either a Zorbax SB-C18 or HALO column using linear gradients of 0.1% acetic acid in nanopure water (v/v%) and HPLC-grade acetonitrile. Preparative high-performance liquid chromatography (prep-HPLC) purification was performed on a Beckman Coulter System Gold HPLC with a 127 solvent pump module and 166P detector set to detect at 210 nm. A linear gradient from 95:5 (v:v%) 0.1% AcOH in H_2O (v:v%): MeCN to 5:95 (v:v%) 0.1% AcOH in H_2O (v/v%): MeCN over 9-14 minutes was used for separation. Absorbance measurements were collected on a Varian Cary 50 Scan UV/Vis spectrophotometer and analyzed using Cary WinUV software in nanopure water. Fluorescence data were taken on a Horiba Jobin Yvon Fluorolog-3 fluorometer using a 450 W Xe lamp and right-angle detection.

Supplementary Note 2. Signal intensity as a function of relaxivity in phantom MRI (Figure 2B). During MRI acquisition time, T_1 weighting is accomplished by use of a short repetition time (TR) relative to the T_1 of the imaged sample or tissue. After several pulses (dummy pulses) a steady state magnetization is established which has an intensity (M_{ss}) relative to the maximum signal intensity (M_0) of: $\frac{M_{ss}}{M_0} = \frac{(1-e^{-TR/T_1})sin\alpha}{(1-e^{-TR/T_1}cos\alpha)}$, where α = excitation flip angle. The images acquired for Figure 2B were obtained using a fast spin echo sequence (α=90º) with a TR of 500 ms. T_1 of the PBS was measured as 2,770 ms. The molar T_1 relaxivity (r_1) of **chex-MM** was found to be 0.208 $mM^{-1}s^{-1}$ and the molar relaxivity of **P1** was found to be 0.318 $mM^{-1}s^{-1}$. Thus for the three samples in Figure 2B, PBS, 10 mM **chex-MM** in PBS, and 10 mM **P1** in PBS, the T_1's of the samples were: $1/T_1 = 1/T_{1PBS} + r_1*(10\ mM)$ which comes to 2770 ms (PBS), 410 ms (**chex-MM**), and 282 ms (**P1**). This results in M_{ss}/M_0 values for the three samples of 0.165 (PBS), 0.704 (**chex-MM**), and 0.830 (**P1**). Normalizing the intensity of PBS to 1, this gives relative signal intensities of 4.26 (**chex-MM**) and 5.03 (**P1**). However, this relative signal intensity does not include decay due to T_2. The RARE (fast spin echo) sequence used a four-echo train with the central k-space echo at an echo time (TE) of 8.9 ms. Signal intensity loss due to T_2 loss is given my $M_{T2}/M_{ss} = e^{-TE/T2}$. The T_2 of PBS is 325 ms. Molar T_2 relaxivity (r_2) of

chex-MM was found to be 0.300 $mM^{-1}s^{-1}$ and the molar relaxivity of P1 was found to be 0.821 $mM^{-1}s^{-1}$. Thus for the three samples in Figure 2B, PBS, 10 mM **chex-MM** in PBS and 10 mm **P1** in PBS, the T_2's of the samples were: $1/T_2 = 1/T_{2PBS} + r_2*(10\ mM)$ which comes to 325 ms (PBS), 165 ms (**chex-MM**), and 89 ms (**P1**). Thus T2 signal loss for this sequence in each sample resulted in $M_{T2}/M_{ss} = 0.97$ (PBS), 0.95 (chex-MM), and 0.90 (P1). Normalizing PBS to 1 and taking into account the steady state magnetization, this results in final signal intensities of 4.17 (**chex-MM**) and 4.67 (**P1**), a bit higher than the measured values, but consistent with a 12% contrast enhancement seen with **P1** over **chex-MM**. Note that the T_2 decay calculation does not take into account the multiple echo train, but only includes the first echo, which should dominate the signal intensity in the center of k-space.

Supplementary Methods

Synthetic methods. All reagents and solvents were purchased from Aldrich or VWR unless otherwise indicated. Bis-spirocyclohexylnitroxide-*N*-hydroxysuccinimidyl (NHS) ester[3-5], 3-aminopropyl azide[6], *exo*-norbornene alkyne-*branch*-NHS ester[7], and Grubbs 3rd generation bispyridyl catalyst were synthesized according to previously reported literature procedures[8]. Anhydrous, deoxygenated dichloromethane (DCM) and tetrahydrofuran (THF) were used from solvent purification columns (JC Meyer).

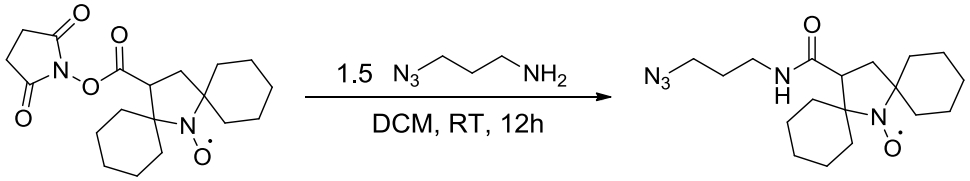

3

Bis-spirocyclohexylnitroxide-propyl-azide 3. Bis-spirocyclohexylnitroxide-*N*-hydroxysuccinimidyl (NHS) ester (60 mg, 0.17 mmol) was added to a vial containing 3-aminopropyl azide (80 µL of 3M solution in toluene, 0.24 mmol) in 1 mL dry DCM. The reaction was stirred for 1 hour, then transferred to a silica gel column and purified via flash chromatography with 5% methanol in DCM. Product containing fractions were determined by LC-MS, combined, dried over $MgSO_4$, and condensed on a rotary evaporator. The yellow residue was dried under vacuum to give the desired product as a yellow oil in 95% yield. ^{1}H NMR is provided in Supplementary Fig. 13. ^{1}H NMR (400 MHz, CD3OD, r.t.): δ 1.36 (s, 2H), 1.62 (m, 5H), 2.24 (s, 2.2H), 2.77 (m, 3H), 3.40 - 4.15 (m, 12H), 4.66 (s, 1.5H), (6.39 (s, 0.1H). DART-HRMS calculated for $C_{18}H_{30}N_5O_2$ $[M+H]^+$ 349.247, observed 349.2467.

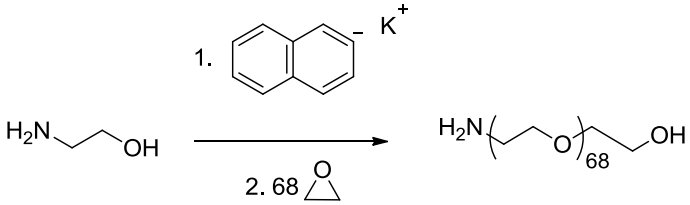

Poly(ethylene glycol) monoamine (PEG-NH_2) synthesis.

Reaction Setup: A lecture flask of ethylene oxide (EO) was connected in series to a graduated vessel (for EO drying, *vide infra*), and a reaction flask. Teflon tubing was used to connect the vessels, all stir bars were pyrex coated, and all joints were lubricated with fluorinated grease. All portions of the reaction setup were carefully kept under nitrogen at all times and isolated from one another until otherwise indicated. A blast shield was placed in front of any vessel containing EO. Supplementary Fig. 12 shows a picture of the reaction setup.

Potassium naphthalenide initiator: An oven-dried 100 mL Shlenck flask equipped with a pyrex stirbar was evacuated and refilled with nitrogen three times. Potassium metal (0.92 g, 23.6 mmol) was cut under mineral oil and transferred with tweezers to a vial containing dry cyclohexane. Potassium was transferred to a second vial of clean cyclohexane to remove any residual mineral oil, and then added quickly to the Schlenk flask. Residual cyclohexane was removed by vacuum (30 min). Napthalene (3.30 g, 25.8 mmol, 1.1 eq) was then added to the

Schlenk flask, which was briefly evacuated and refilled with nitrogen. Dry THF (23.6 mL) was added; the solution immediately began to turn dark green as potassium dissolved. The flask was covered with aluminum foil and stirred at room temperature for 2 h. The initiator concentration was tested by titration against 0.10 mL (1.3 mmol) isopropanol in 10 mL THF. After adding 1.40 mL of initiator, the dark green initiator color remained for over ten seconds, indicating a concentration of 0.93 M. The initiator was stored in the aluminum covered Schlenk flask for up to three days before use.

Calcium hydride (1 g) was added to the drying vessel (labeled b in Supplementary Fig. 12). An ice bath was placed around the drying vessel, the EO tank was opened slowly and EO was allowed to condense in the drying vessel. Once 22 mL (440 mmol) of liquid EO had accumulated, the EO lecture flask was closed, isolated from the drying vessel, and removed from the hood. The ice bath was maintained around the drying flask as redistilled aminoethanol (0.40 mL, 6.6 mmol) and dry THF (45 mL) were added to the reaction flask through a rubber septum. Potassium naphthalenide solution (7.10 mL of 0.93 M, 6.6 mmol) was added, and the mixture became white and cloudy; the precipitated potassium aminoethanoxide was washed from the flask walls with 5 mL THF. The ice bath was then removed from the drying vessel and placed around the reaction flask. The drying vessel was opened to the reaction flask, and the EO was allowed to boil and slowly distill into the reaction flask. Once the drying flask was empty, the reaction vessel was sealed, the ice bath was removed, and the reaction was allowed to warm to room temperature. The polymerization was stirred at room temperature for 72 h. After this time, 6.6 mmol of hydrochloric acid (5.3 mL of 1.25M HCl in methanol) was added dropwise to the reaction. The flask was then opened to air and stirred for 1 h. The reaction mixture was then poured directly into 700 mL of cold diethyl ether and stored at -20° C for 1 h. The white precipitate was vacuum filtered, redissolved in 70 mL of toluene, and precipitated in cold ether again. After a second filtration, the polymer was vacuum dried overnight to remove all residual solvent, providing a powdery white solid in 92% isolated yield. ^{1}H NMR spectrum is shown in Supplementary Figure 14. ^{1}H NMR (400 MHz, CD3OD, r.t.): δ 2.84 (t, 2H), 3.63 (m, 244H). MALDI-TOF calculated for $C_{136}H_{275}NNaO_{68}$ $[M+Na]^+$ 3034.802, observed 3034.7640.

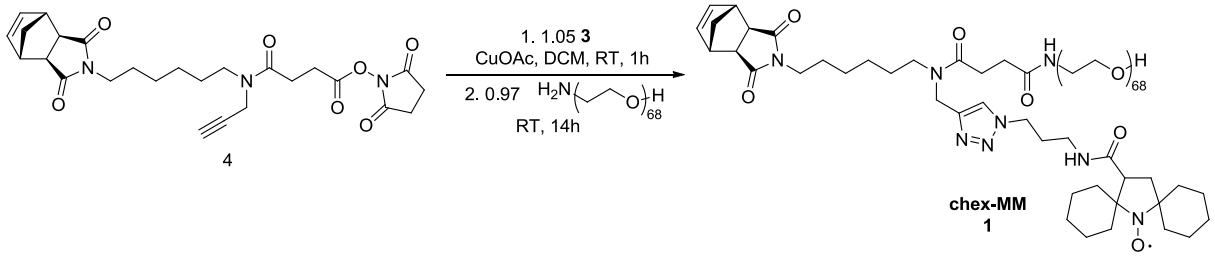

Norbornene-PEG-*branch*-chex MM (1). Compound 4 (37.4 mg, 75 mmol) was added to a vial with azide 3 (27.6 mg, 79 mmol) and 3 mL dry DCM under N_2. A spatula tip of CuOAc was added and the vial was flushed with N_2. After five minutes, LC/MS analysis of the reaction indicated nearly complete conversion of **2** to the intermediate triazole-*branch*-NHS compound. Solid PEG-NH_2 (220 mg, 73 mmol) was then added to the reaction and the mixture was stirred for 14 h. The entire reaction mixture was dried on a rotary evaporator, redissolved in MeOH (3 mL), passed through a 0.4 □m Nylon syringe filter, and subjected to prep-HPLC. The pure fractions containing chex-MM were condensed with a rotary evaporator. The resulting residue was dissolved in dichloromethane (DCM), dried over Na_2SO_4, condensed on a rotary evaporator, and dried overnight under vacuum to yield a light yellow solid in 65% yield. MALDI spectrum is shown in Supplementary Fig. 1, and ^{1}H NMR is provided in Supplementary Fig. 15.

^{1}H NMR (400 MHz, CD3OD, r.t.): δ 1.27 (m, 6H), 1.52 (m, 6H), 2.14 (s, 10H), 2.55 (s, 2H), 2.69 (m, 3H), 3.28 (s, 2H), 3.48 (m, 6H), 3.66 (m, 220H), 3.85 (t, 2H), 6.30 (s, 2H), 6.51 (s, 1H).

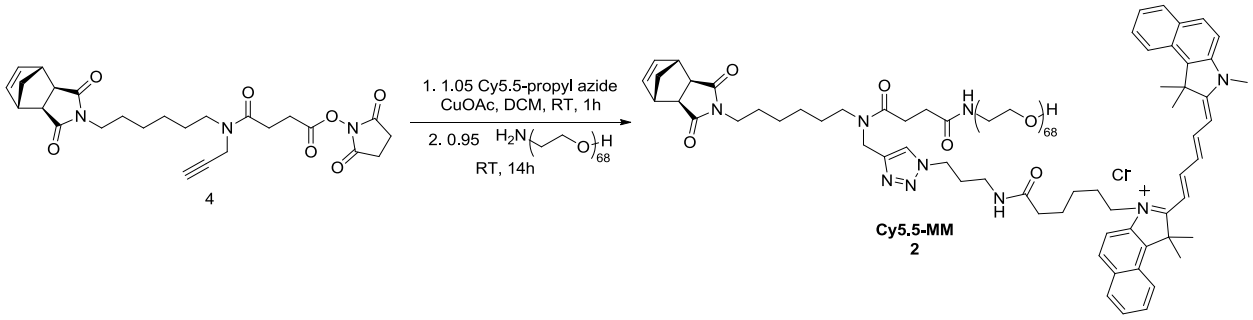

Norbornene-PEG-*branch*-Cy5.5 MM (2). Compound 4 (1.3 mg, 2.6 mmol) was added to a vial with Cy5.5-propyl azide (Kerafast, 2 mg, 2.8 mmol) and 1 mL dry DCM under N_2. A spatula tip of CuOAc was added and the vial was flushed with N_2. After five minutes, LC/MS analysis of the reaction indicated nearly complete conversion of **4** to the intermediate triazole-*branch*-NHS compound. Solid PEG-NH_2 (7.7 mg, 2.5 mmol) was then added to the reaction and the mixture was stirred for 14 h. The entire reaction mixture was dried on a rotary evaporator, redissolved in MeOH (0.7 mL), passed through a 0.4 µm Nylon syringe filter, and subjected to prep-HPLC. The pure fractions containing Cy5.5-MM were condensed with a rotary evaporator. The resulting blue residue was dissolved in dichloromethane (DCM), dried over Na_2SO_4, condensed on a rotary evaporator, and dried overnight under vacuum to yield a blue solid in 77% yield. The MALDI spectrum is shown in Supplementary Fig. 1, and the ^{1}H NMR is shown in Supplementary Fig. 16. ^{1}H NMR (400 MHz, CD3OD, r.t.): δ 1.15-1.29 (m, 7H), 1.42-1.58 (m, 8H), 1.76 (s, 2H), 2.20-2.55 (m, 18H), 2.64 (d, 4H), 3.24 (m, 6.5H), 3.39 (m, 6.5H), 3.63 (m, 305H), 4.18 (s, 2H), 4.40 (m, 2H), 4.54 (s, 2H), 6.25 (m, 3H), 6.37 (m, 1H), 6.72 (m, 1H), 7.39 (t, 2H), 7.48 (m, 2H), 7.61 (t, 2H), 7.93 (m, 6H), 8.07 (m, 2H).

Supplementary References

1 Rowland, M., Benet, L. Z. & Graham, G. G. Clearance Concepts in Pharmacokinetics. *J. Pharmacokinet. Biopharm.* **1**, 123-136, (1973).

2 Burts, A. O., Li, Y. J., Zhukhovitskiy, A. V., Patel, P. R., Grubbs, R. H., Ottaviani, M. F., Turro, N. J. & Johnson, J. A. Using EPR To Compare PEG-branch-nitroxide "Bivalent-Brush Polymers" and Traditional PEG Bottle-Brush Polymers: Branching Makes a Difference. *Macromolecules* **45**, 8310-8318, (2012).

3 Rajca, A., Wang, Y., Boska, M., Paletta, J. T., Olankitwanit, A., Swanson, M. A., Mitchell, D. G., Eaton, S. S., Eaton, G. R. & Rajca, S. Organic Radical Contrast Agents for Magnetic Resonance Imaging. *J. Am. Chem. Soc.* **134**, 15724-15727, (2012).

4 Kirilyuk, I. A., Polienko, Y. F., Krumkacheva, O. A., Strizhakov, R. K., Gatilov, Y. V., Grigor'ev, I. A. & Bagryanskaya, E. G. Synthesis of 2,5-Bis(spirocyclohexane)-Substituted Nitroxides of Pyrroline and Pyrrolidine Series, Including Thiol-Specific Spin Label: An Analogue of MTSSL with Long Relaxation Time. *J. Org. Chem.* **77**, 8016-8027, (2012).

5 Paletta, J. T., Pink, M., Foley, B., Rajca, S. & Rajca, A. Synthesis and Reduction Kinetics of Sterically Shielded Pyrrolidine Nitroxides. *Org. Lett.* **14**, 5322-5325, (2012).

6 Lewis, W. G., Magallon, F. G., Fokin, V. V. & Finn, M. G. Discovery and characterization of catalysts for azide-alkyne cycloaddition by fluorescence quenching. *J. Am. Chem. Soc.* **126**, 9152-9153, (2004).

7 Johnson, J. A., Lu, Y. Y., Burts, A. O., Xia, Y., Durrell, A. C., Tirrell, D. A. & Grubbs, R. H. Drug-Loaded, Bivalent-Bottle-Brush Polymers by Graft-through ROMP. *Macromolecules (Washington, DC, U. S.)* **43**, 10326-10335, (2010).

8 Love, J. A., Morgan, J. P., Trnka, T. M. & Grubbs, R. H. A practical and highly active ruthenium-based catalyst that effects the cross metathesis of acrylonitrile. *Angew. Chem., Int. Ed.* **41**, 4035-4037, (2002).